Available online at: http://ijmt.ir/browse.php?a code=A-10-165-1&sid=1&slc lang=en

# An Investigation into the Pull-out Failure Mechanisms of Suction Caissons

# Mostafa Zeinoddini<sup>1\*</sup>, Mahmood Nabipour<sup>2</sup>, Hamid Matin Nikoo<sup>3</sup>

- \*1 Civil Eng. Department, K.N.Toosi University of Technology; zeinoddini@kntu.ac.ir
- <sup>2</sup> Civil Eng. Department, K.N.Toosi University of Technology; mnabipour7@gmail.com
- <sup>3</sup> Civil Eng. Department, K.N.Toosi University of Technology; hamidmatin@sina.kntu.ac.ir

## **ARTICLE INFO**

## Article History: Received: 15 Jun. 2014 Accepted: 3 Aug. 2015

Keywords:
offshore structures
suction caisson
pull-out capacity
drained failure mode
undrained failure mode

#### **ABSTRACT**

This paper reports results from an investigation into the suction caissons failure mechanisms under vertical pull-out loads. An insight to the failure mechanisms of suction caissons paves the path for developing analytical solutions to their pull-out capacity. The numerical models of suction caissons have first been calibrated by and verified against several experimental data from other researches. The verified numerical models have then been used to obtain the pull-out response of suction caissons under a variety of conditions. In the current research, as a key finding, four distinctive failure modes are introduced for the vertical pull-out of suction caissons. They vary from local modes, with caissons of low penetration in weak soils under drained conditions, to global modes, with caissons of sufficient penetration in stronger soils under undrained conditions. In general, with local modes the failure surface is close to caisson walls. With global modes, the failure surface moves away from the caisson walls and well extends in the surrounding soil. The pull-out capacity is highly reliant on the mode of the failure and on the whole it increases as the mode moves from local to global.

## 1. Introduction

Exploration and development of oil fields growingly move to deeper waters and consequently to more severe environments. Offshore rigs now reach water depths in the 1000 to 3000m range. Offshore structures such as floating platforms, tension leg platforms and guyed towers are inevitably subject to sever environmental conditions. They produce great uplift forces (in many occasions as tensile) in the foundation. In some tension leg platforms, pull-out forces of the order of 20 to 70MN have been reported [1]. Suction caissons have proved themselves as a novel method of anchoring production platforms in deep waters. They have been designed as an appropriate alternative for rig foundations and to resist large pull-out loads. They have also been employed for many types of marine structures.

Suction caissons are hollow cylinders capped at their top but open at the bottom (Figure 1). Their installation is achieved by a combination of self-weight (or direct loading) and suction (or under pressure). They have become ever more attractive due to cost savings associated with offshore installation activities. They are easier to install than impact driven piles and can be used in water depths well beyond where pile driving becomes infeasible. Suction caissons have higher load capacities than drag

embedment anchors and can be inserted reliably at pre-selected locations and depths with minimum disturbance to the seafloor environment and adjacent facilities [2].

Whilst pile design procedures have evolved from old long-lasting onshore experience and theory, design guidelines for suction caissons have yet to be worked out. There are no accepted procedures, like the API guidelines for piles, nor are there enough amounts of published data.

One of the critical aspects with suction caissons is their ability to resist pull-out loads, which may be applied under extreme environmental conditions. Rate of loading is another issue influencing the response of suction caissons. The typical loading on suction caissons consists of random variations about some mean value. This results in a complex flow regime within the soil matrix. Depending on the loading rate ratio to the rate of fluid flow within the soil matrix (degree of drainage) the suction caisson behaviour will show considerable variations. Therefore, drainage condition dominates the response of the suction caisson.

computations.

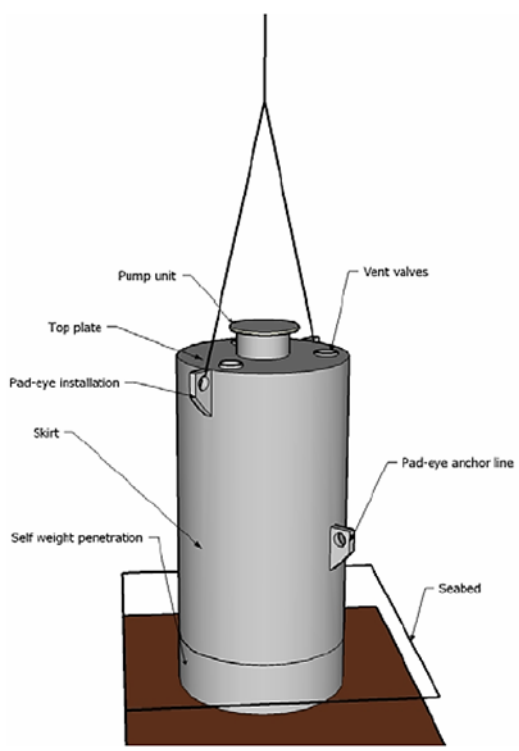


Figure 1: Schematic view of a suction caisson [3]

A number of researchers have studied the behaviour

of suction caissons under various loading and drainage conditions. Small-scale and full-scale field tests on caissons were carried out to determine their installation characteristics and their axial and lateral load capacities [4-6]. Field tests provide valuable geotechnical information relevant in the design of caissons, but they are expensive and time-consuming. Geotechnical centrifuge tests on model suction caissons were performed to simulate the stress conditions and soil response at the field scale [7,8]. These are also quite costly and remain subject to various limitations. Laboratory testing of model suction caissons under 1-g and controlled laboratory conditions were employed to investigate performance of the caissons under a variety of conditions [9-14]. Numerical simulation is another approach being chosen by some researchers to investigate the behaviour of suction caissons under different loading and drainage conditions [15-18]. They carried out axisymmetric and three-dimensional numerical modelling to determine the capacity of suction caissons. A number of researcher [used the commercial finite element code Abaqus [15,16,19]. El-Gharbawy and Olson [17] used the commercial

Some other researchers selected analytical approaches consisting of a combination of plasticity models and experimental results to express the load bearing capacity of suction caissons [7,8,18].

finite element code PLAXIS [20] for geotechnical

Understanding the failure mechanisms of suction caissons under different conditions is utterly imperative for developing analytical solutions to their

load bearing capacity. The current study follows a numerical approach to investigate the failure behaviour of suction caissons subject to the pull-out loading. Utilising a verified numerical model to predict the failure mechanisms of a suction caisson may be regarded as a novel approach to these types of problems. An insight to the failure mechanisms of suction caissons paves the path for developing analytical solutions to their pull-out capacity.

The normal practice is to identify the failure modes from physical observations. With the numerical modelling it is possible to examine a wide range of different soil/caisson/drainage conditions and to monitor the responses very inside the caisson and in the embedded zones which are extremely difficult or even impossible to comprehend in a physical sense

The employed finite element models have been calibrated against available experimental pull-out data in sands and clays. The calibrated models have further been verified against some other available test results. The verified models have then been employed to examine the behaviour of the suction caissons and to study their failure mechanisms with different soil/caisson/drainage configurations against vertical pull-out loading.

# 2. Calibration/verification of the numerical model

# 2.1. Modelling premises

Simulation of non-linear and time dependent responses of soils requires advanced numerical models. With suction caissons, the saturated soil has to be modelled as a two-phase medium composed of solid (soil skeleton) and pore-fluid (water) phases. In the current study the two dimensional finite element program PLAXIS Version 7.2 has been used to examine the behaviour of suction caissons. PLAXIS is particularly designed for analysing deformations and stability in geotechnical projects.

The soil elasticity has been defined by Young's modulus (*E*) and Poisson's ratio (v). Non-linear behaviour of the solid phase has been described by means of a classical elasto-perfect plastic soil model. A Mohr-Coulomb model has been exercised to simulate these soil behaviours. Mohr-Coulomb yield condition is an extension of Coulomb's friction law to general states of stress. In fact, this condition ensures that Coulomb's friction law is obeyed in any plane within a material element. The full Mohr-Coulomb yield condition can be defined by three yield functions when formulated in terms of principal stresses [21]:

$$f_{1} = \frac{1}{2} |\sigma'_{2} - \sigma'_{3}| + \frac{1}{2} (\sigma'_{2} + \sigma'_{3}) \sin \varphi - c \cos \varphi \le 0$$

$$f_{2} = \frac{1}{2} |\sigma'_{3} - \sigma'_{1}| + \frac{1}{2} (\sigma'_{3} + \sigma'_{1}) \sin \varphi - c \cos \varphi \le 0$$

$$f_{3} = \frac{1}{2} |\sigma'_{1} - \sigma'_{2}| + \frac{1}{2} (\sigma'_{1} + \sigma'_{2}) \sin \varphi - c \cos \varphi \le 0$$
(1)

The two plastic model parameters appearing in the vield functions are the well-known friction angle (Φ) and the cohesion (c). These yield functions together represent a hexagonal cone in principal stress. The minimum normal stress has been bounded by a tension cut-off limit introduced in the model for the soil part. In addition to the yield functions, three plastic potential functions are defined for the Mohr-Coulomb model. The plastic potential functions contain a third plasticity parameter. The dilatancy angle (φ) in the plastic potential is required to model volumetric strain plastic increments (dilatancy) as observed for dense soils.

The employed Mohr-Coulomb soil plastic model is relatively versatile and, as it will be shown later, provides reasonable agreements with the test results. It should be mentioned that a modified Cam-Clay plastic model has also been examined with some models. In general, more conservative pull-out capacities have been emerged from models with a Mohr-Coulomb soil plastic criteria in comparison to those from corresponding models with the modified Cam-Clay plastic criteria.

Based on the geometry of the problem, a two dimensional axisymmetric model has been chosen to simulate the pull-out behaviour of the caisson. Sixnode triangular elements which provide a second order interpolation for displacements have been used. The element stiffness matrix is evaluated by numerical integration using a total of three Gauss points (stress points). This element type performs well for most types of calculations (PLAXIS Manual). The caisson itself has been modelled by non-porous linear elastic materials with elastic modulus that sufficiently exceed that of the soil.

A key feature with numerical simulation of geotechnical problems containing structural elements is the type and the model of interaction between the soil and the structural elements. A frictional contact algorithm, based on a slide-line formulation that allows for large relative displacements between the caisson wall and the soil, has been considered for the soil/structure interaction. The roughness of the interaction has been modelled by choosing a suitable value for the strength reduction factor  $(R_{int})$  in the interface. This factor relates the interface strength (wall friction and adhesion) to the soil strength (friction angle and cohesion) and characterizes an elastic-plastic model for the soil/structure interactions. The coordinates of each node pair on the wall skin and the adjacent soil body are identical. This means that the interface element has a zero thickness. Each interface element has assigned to it a 'virtual thickness' which is an imaginary dimension used to obtain the material properties of the interface. The stiffness matrix for interface elements is obtained using Newton-Cotes integration points. The position of these integration points (or stress points) coincides with the position of the node pairs. Hence, for the 6node interface elements considered in the current study, a 3-point Newton-Cotes integration is used.

To avoid problems of stress concentration/fluctuation in sharp corners of intersections between the soil elements and the structural elements, interface elements have been extended to some degrees deeper than the caisson tip into the soil body underneath the caisson. For interface elements extended below the caisson edges into the soil body a value of 1.0 has been considered for  $R_{int}$ . The extended part of the interface elements into the soil body should not influence the water flow in the surrounding soil and not to impart effects on the soil strength characteristics. For these reasons, a neutral material setting has been used.

With experimental models, when the soil boundaries are considerably far from the caisson's body, boundary effects on the caisson response can be neglected. Davie and Sutherland [22] and Rao et al. [23] suggested on extents 8 to 10 times that of the caisson's length and radius. In numerical models of suction caissons, the radius and the depth of the soil body have been considered as about 8 to 10 times that of the corresponding dimensions of the caisson. A standard fixity boundary condition has been considered on the soil borders. The vertical boundary line had a horizontal fixity ( $u_x = 0$ ), while the lower horizontal boundary line had a full fixity ( $u_x = u_y = 0$ ). Regarding the hydraulic boundary condition, the phreatic level has been set at the elevation for the free water surface in the soil tank used in the laboratory model tests. Due to the axisymmetric nature of the model, it is assumed that no flow enters or leaves the left soil boundary. The left vertical boundary has, therefore, been set as impervious. The soil boundaries to the right and bottom have been assumed to be too far from the caisson to have significant influence on the results, so they have also been set impervious.

In numerical models of suction caissons, the radius and the depth of the soil body have been considered as about 8 to 10 times that of the corresponding dimensions of the caisson.

The pull-out load has been introduced on top of the caisson and above its walls. This is to eliminate possible flexural performances from the structural elements in the caisson cap. For the soil body a relatively fine meshing has been used in the vicinity of the caisson while, coarser meshes have been utilized elsewhere to reduce the computational efforts. A load advancement number of steps option which is more suitable for cases with possible failure conditions (PLAXIS Manual) has been used for the calculation method.

With drained models no excess pore pressure are generated. This is obviously the case for pulling out the caisson when free drainage possibility has been allowed from the top cap of the caissons. The

employed undrained models allow for a full development of excess pore pressure when the top cap is closed during the pull-out.

It is noted that when the top of the caisson is sealed, due to the incompressibility of the pore water, the volume of the water layer will initially remain unchanged during loading. However, the water might dissipate under long-duration sustained loading. The second order wave actions/currents and the drift forces might be assumed as sustained loads. In contrast, the pull-out caused by the first-order wave takes place in a short period of time, so it is generally expected that the soil response is "undrained". Three key components of i) soil permeability; ii) rate of loading; and iii) caisson characteristics then contribute to the pull-out response. If the permeability coefficient is very high (which is not usually the case for marine sands), the soil response may become drained. If the rate of loading (say pull-out) is very slow the soil has enough time to drain. If the caisson is open-top (which may be the case during decommissioning) it can provide additional ways for water to drain and the soil behaviour inside the caisson gets closer to drained condition (in other words, the open-top caisson does not guarantee drained condition in the whole problem So, in general, the pull-out action especially in clayey soils (where the permeability coefficient is very low) the soil response will be undrained. It means that the water inside the caisson will be trapped and the situation can be assumed as fully undrained [24].

To model a fully undrained situation, therefore, there is no need for a time dependent coupled consolidation analysis. It suffices to perform a fully undrained effective stress analysis using undrained soil strength parameters [11]. The fully undrained and fully drained modellings in Plaxix are not, thus, time or rate dependent analyses.

With a fully drained models the Plaxis assumes that no excess pore pressure is generated. This is the case for the caisson pull-out when free drainage from the top cap of the caisson is allowed.

As will be explained later in Section 2.3, the Abaqus non-linear finite element software (Simulia , 2008) has also used in the current study as a double-check for the Plaxis simulations. It should be mentioned that the Abaqus soil model is rate dependent. For simulating an undrained condition the loads should have had a high rate (rates between 2 to 5 mm/s are used) but for a drained condition the rate was low  $(2\times10^{-4} \text{ to } 5\times10^{-4} \text{ mm/s})$ .

# 2.2. Test data used for calibration/verification

The validity of numerical models, employed in the current study, has been examined by comparing the simulation results with the experimental data available in the literature. The laboratory data used for the

calibration/verification of numerical models are those from [7] and [23].

Obviously the constitutive model parameters will differ depending on the caissons modeled in the validation or the parametric studies. As an example the Mohr-Coulomb and Cam Clay constitutive model parameters used in simulating the experiments from Rao et al. [11] are given in Table 1 and Table 2.

Table 1. Properties of the Mohr-Coulomb soil model in Plaxis

	[11]		
Young's modulus	E	1.5	MPa
Poisson's ratio	ν	0.35	-
Undrained cohesion	$c_u$	1.8	kPa
Friction angle	$\phi$	25	Degree
Dilatancy angle	Ψ	0	Degree
Soil unit weight	γ	16.4	kN/m <sup>3</sup>

Table 2. Properties of the Cam Clay soil model in Plaxis [11]

Modified compression index	λ	0.1	-
Modified swelling index	κ	0.02	-
Cohesion	$c_u$	1.8	kPa
Friction angle	$\phi$	25	Degree
Dilatancy angle	Ψ	0	Degree
Soil unit weight	γ	16.4	kN/m <sup>3</sup>

#### 2.3. Calibration/verification results

Experimental results from Rao et al. [11] have been used for calibration of numerical models concerning the interface ratio  $(R_{int})$ . In the absence of detailed data, PLAXIS suggests R<sub>int</sub> values in order of 2/3 for a sand-steel contact and 1/2 for the clay-steel contact. Acquiring detailed data on the extent and the type of soil/structure interaction during the pull-out of the caisson is achievable, even though special experimental provisions become necessary. However, the previously referenced experiments, which have been used for the calibration and verification of the numerical models in the current study, were lacking such detailed information. To obtain a fitting evaluation of  $R_{int}$  and for the purpose of calibration, different values of  $R_{int}$  have been examined against the corresponding experimental data [11]. Numerical models of caissons having aspect ratios of 1, 1.5 and 2 respectively in undrained clays have been examined. Figure 2 presents for a typical load-displacement response obtained for one of the three geometries chosen for the calibration purposes. Based on the calibrations attempts it has been found that for clays a value of  $R_{int} = 0.5$  and for sands  $R_{int} = 0.4$  presents better consistency with the experimental results. Accordingly, henceforth, these values have been used suction caissons modelling. acknowledged, however, that unique values of  $R_{int}$  are not applicable in all cases and the ratio may vary depending on the caisson's skin roughness, soil characteristics, drainage conditions and even down the caisson's depth.

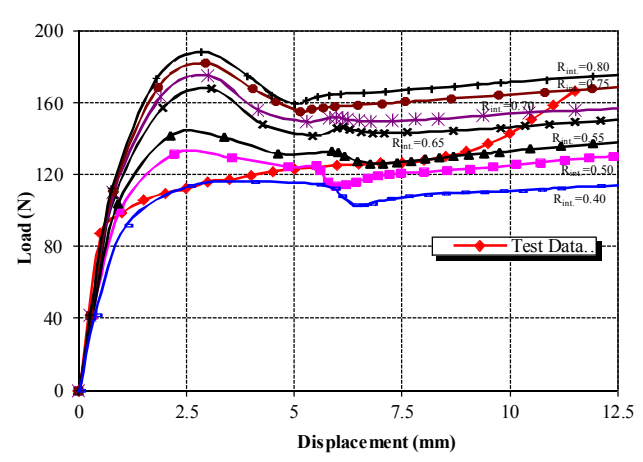


Figure 2. Calibration of numerical models (aspect ratio of 2) in undrained clay against different values of  $R_{int}$  from the current study and test data from [11].

Pull-out behaviour of calibrated numerical models has furthermore been verified using other experimental data. The verification has been carried out by means of test data from Iskander et al. [26] for sand models and El-Gharbawy and Olson [25] for clay models. Both drained and undrained conditions have been considered. In Figures 3 and 4, for instance, the experimental and the numerical load-displacement curves for two of the examined cases are compared. Rao et al. [11] carried out a series of 1-g tests on

Rao et al. [11] carried out a series of 1-g tests on suction caissons with different aspect ratios (L/D) to get an estimate of their pull-out capacity in soft clays (similar to those in the Indian waters). The caisson's dimension and the soil property in three out of nine series of their experiments are listed in table 3:

Table 3. Caisson's dimension and the soil property in three out of nine series of their experiments

$$D = 75 \text{ mm}$$
  
 $LI = 0.4, 0.6 \text{ and } 0.8$   
 $S_r = 0.95, 0.96 \text{ and } 0.97$ 

L/D = 1.0, 1.5 ar $c_u = 1.8, 3.6, 5.8$ 

 $c_u = 1.8, 3.0, 3.8$  $\gamma = 16.4, 16.45, 10.7 \text{ Kin/m}$ 

El-Gharbawy and Olson [24] conducted 1-g pull-out tests on caisson models with different aspect ratios (2 to 12) in kaolin clays under drained and undrained conditions.

They tried to evaluate the response of the suction caisson foundations for TLPs in the Gulf of Mexico in deep waters of 2000 to 3000m. The caisson's dimension and the soil property in their tests were:

$$D = 100 \text{ mm}$$
  $t = 3.125 \text{ mm}$   $L/D = 4 \text{ and } 6$   $\varphi = 27.8^{\circ}$   
 $PL = 27\%$   $LL = 57\%$   $c = 0.1 \text{ KN/m}^2$ 

Iskander et al. [26] performed 1-g tests in sand to investigate the variation of the pore pressure during the penetration and subsequent pull-out of the suction caisson models. They used Oklahoma sand in their experiment which is quite fine and rounded. The caisson's dimension and the soil properties in their tests were:

$$L = 194 \text{ mm}$$
  $D = 110 \text{ mm}$   $t = 5 \text{ mm}$   $\phi = 41^{\circ}$ 

 $G_s = 2.65$  k = 0.01 mm/day  $e_{max} = 0.70$   $e_{min} = 0.46$   $C_c = 1.1$   $C_u = 1.6$  KN/m<sup>2</sup>  $\gamma_{d max} = 17$  KN/m<sup>3</sup>  $\gamma_{d min} = 15.3$ KN/m<sup>3</sup> Based on the above described calibration and verification attempts, it can be assumed that the employed numerical models are able to predict the behaviour of the suction caissons in different soil types and drainage conditions within acceptable accuracies.

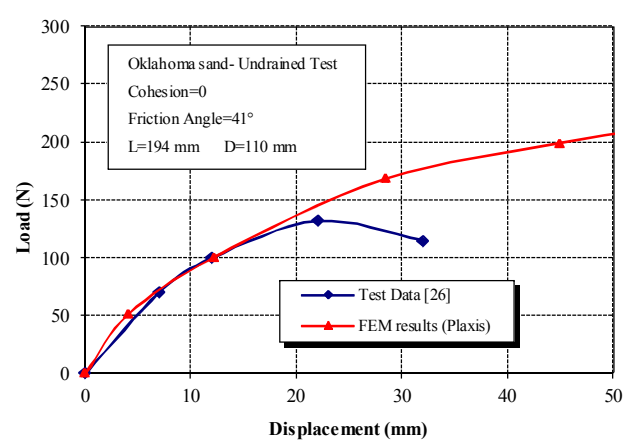


Figure 3. Verification of numerical results against experimental data for suction caisson models in sand under undrained conditions.

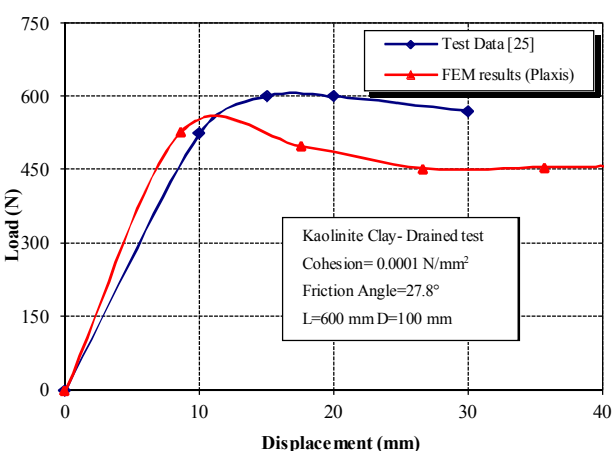


Figure 4. Verification of numerical results against experimental data for suction caisson models in clay under drained conditions (Kaolinite clay, drained condition, L=600 mm, D=100 mm, c =1 kPa,  $\varphi$  =27.8°,  $\psi$ =0, E=1 MPa, v=0.35).

It was noted that with  $R_{int} = 0.5$ , Figure 2 showed a reasonable agreement between relatively numerical and experimental data. However, with respect to the load-bearing path, the experimental and numerical results were not in complete agreement. The experimental data in Figure 2 shows a monotonic increase in the capacity while the numerical model does not. Also in Figure 3 peak of the two curves do not match, and in Figure 4 the residual load bearings are different. First of all it would be a high expectation that a numerical model can give exact predictions for complicated geotechnical problems such as suction caisson, because of the many unknown parameters involved in the real physics of the problem. Secondly the differences in each case should be interperated separately. For example, the numerical

response in Figure 2 demonstrates: (i) an initial monotonic increase in the load bearing, which is larger than the corresponding experiment, (ii) a drop in the capacity at about 5 mm displacement, and (iii) a subsequent increase in the load bearing. The drop in capacity with the numerical responses is seemingly caused by the local tensile failure at the bottom of the soil plug due to the tension-cut-off limit introduced to the numerical model. The subsequent increase in the capacity is believed to be caused by the changes in the pore pressure due to increase in the caisson displacement. Effective stresses in the soil body are then proportionally intensified and hence after an early drop, the caisson regains resistance to the pullout. This can be recognised by the slight hardening trend in the numerical response which keeps continuing in displacements larger than those shown in the figure. The experimental curves so appear to have demonstrated similar tri-stage responses (a peak, a drop and hardening), but they occurred earlier and over a smooth path.

It is also noted that new versions of the Plaxis, rather than the 7.2 version, have now been made available which enable 3D and dynamic analyses. In general, 3D models of the Plaxis are not as accurate as 2D models [27], so ultimate limit states (such as safety factors or bearing capacities) may be overestimated. For this reason in the current study a 2D axisymetric modelling approach based on Plaxis-7.2 is used. In addition, Abaqus 6.10 non-linear finite element software [19] has been employed for the 3D modelling of the quasi-static pull-out behaviour of the suction caissons to ensure the accuracy of the modelling. In general, the predictions obtained from the two software in the current study have been in reasonable agreements.

The 3D Abaqus model of the suction caisson consists of a soil domain modelled by first order hybrid or porous solid (C3D8P and C3D8H) elements. The skirt of the suction caisson is modelled using S4 shell elements. Elements type R3D3 are used for the caisson lid. Owing to the geometrical symmetry of the problem only one quarter of the geometry is modelled. The radius of the soil body in the Abaqus models is about 5 times of the caisson radius (Figure 5). A Mohr-Coulomb plasticity model with a non-associated flow rule is assigned to the soil elements. The suction caisson is considered in an in-situ condition so the installation phase is not modelled. Two types of Abaqus analyses are performed. The first one, the soil analysis, is a rate-dependent, coupled soil/structure analysis and explicitly simulates both the drained and undrained conditions. The second one is a Riks type of analysis. Extra details can be found in Zeinoddini et al [28].

The predictions of the Abaqus 3D models are verified against a number of experimental data in Figure 6. The figure depicts the results from simulation of a

laboratory model of suction caisson with D=75mm, L=75mm, installed in an over-consolidated clay soil, under pull-out loading and undrained conditions [11]. The predictions from both the soil and the Riks analyses are given in the figure. Relatively good agreements can be seen between the two analysis methods and the experimental data.

It is noted that the term "Static Analysis" in Figure 6 stands for the Riks method results. Riks method uses an arc length solution scheme for tracing the nonlinear equilibrium path near an unstable state or beyond a limit or bifurcation point. The Riks method provides the possibility of tracing the behaviour up to the collapse and in the post collapse conditions [19]. However, it is not possible to incorporate the Riks method into a multiphase medium such as soils for a coupled soil/structure analysis. In spite of this, with introducing a layer of weaker soil on the interior and exterior wall skins of the caisson and below its lid, the soil/caisson interactions can be implicitly modelled. This is similar to that used by Supachawarote et al. [29] for the analysis of inclined pull-out capacity suction caissons. Extra details can be found in [28].

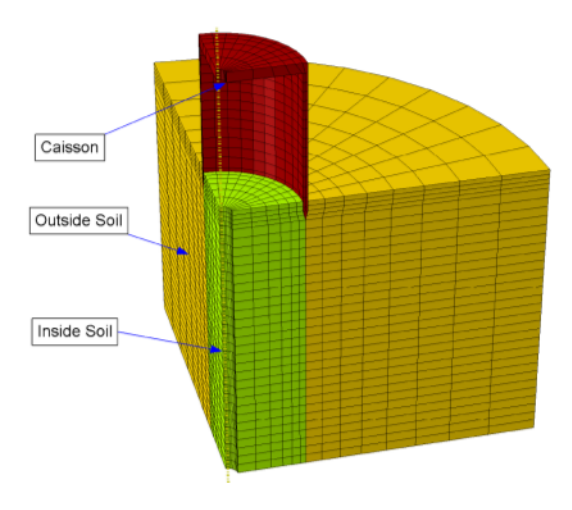


Figure 5. A view of the 3D Abaqus finite element model of a suction caisson.

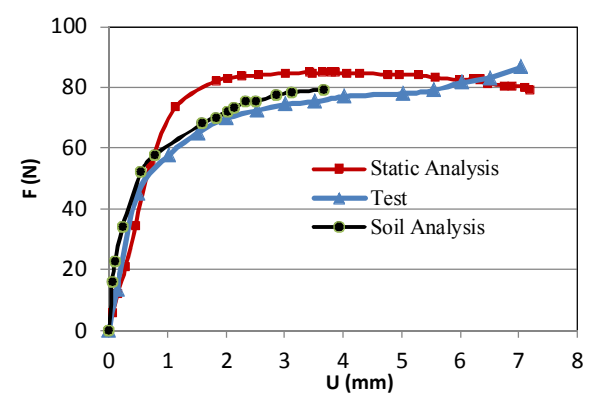


Figure 6. Comparing the results of the Abaqus models from the soil and Riks analyses (current study) with test data (Rao et al., 1997).

# 3. General results on pore pressure variations

Figure 7 shows the situation with pore water pressure in an undrained model in clay prior to and after the pull-out loading. Figure 7 (left) gives the distribution of the total water pressure generated in the model after defining the phreatic level and before introducing the pull-out load. <u>Simple</u> signs in the figure indicate on <u>total</u> initial pressure. The size of the signs signifies the relative magnitude of the pressure.

Figure 7 (right) gives a snapshot of the excess pore water pressure distribution during simulation of the pull-out. It is noted that the pressure distribution would vary depending on the pull-out advancement. Arrowed signs in this figure display the distribution of the excess pore pressure. The length of the arrows indicates the relative magnitude of the pore pressure. The arrows' orientation signify the pressure sign. Outward arrows, similar to those in Figure 7 (right), indicate on suction (and vs.). In Figure 7 (right) the suction build up, subsequent to the pull-out loading, can be noticed inside and around the caisson. Negative excess pore pressures are produced inside the caisson, but they gradually fade away far-off the caisson. As it may notice the largest suction occurs inside the caisson and slightly above the caisson tip. It gradually dissipates far away from the caisson.

Figure 7 is just indicative and from one of the examined models. In fact, the intensity and the distribution of the negative excess pore pressures depend on the level and the rate of the applied pull-out load, the soil permeability, the caisson geometry and its penetration in the soil. Figure 8 shows the excess pore pressure values across a line AA' in the mentioned model.

------

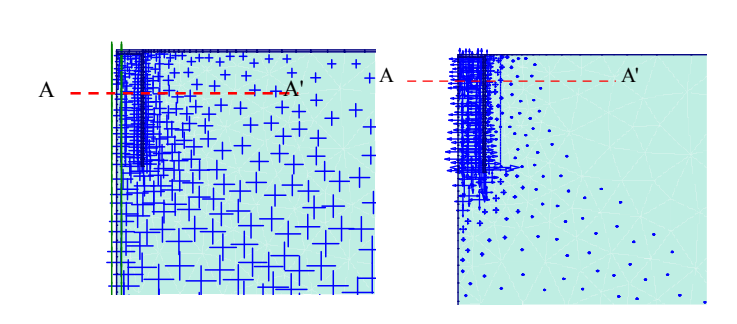


Figure 7. Variation of pore water pressure with an undrained model prior to the pull-out (in left where hydrostatic pressures are given and the water surface is also shown) and after the pull-out loading (in right where the excess pore pressures are shown and they gradually dissipate far away from the caisson.



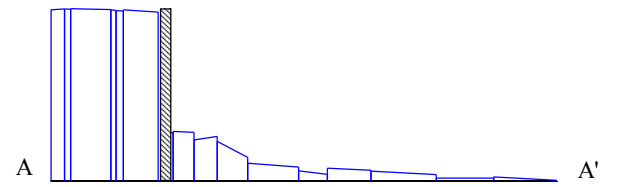


Figure 8. Variation of water pressure with an undrained model prior to the pull-out (above) and after the pull-out loading (below) across line AA' (see Figure 7). The ordinate present the pore water pressure whilst the abscissa displays the horizontal distance.

# 4. Failure modes observed with suction caissons subject to pull-out loading

A variety of numerical suction caisson models with different "soil/caisson/drainage" characteristics have been examined under vertical pull-out loading. Four distinctive load-displacement behaviours have been identified, each of which has appeared to be "soil/caisson/drainage" associated to a certain category and has been found to lead to a specific failure mode. These failure modes are schematically depicted in Figure 9, which shows free body diagrams in the soil and on the caisson at failure stage. It should be mentioned that failure modes 1, 2 and 4 are similar to those already defined by Steensen-Bach [10]. The failure mode 3 is an outcome of the current study. Another important result of the current study, as mentioned above, is that each failure modes have been found identical to be of "soil/caisson/drainage" categories and loaddisplacement behaviour. Characteristics of these "soil/caisson/drainage" categories, their related pullout behaviour and associated failure modes are illustrated below.

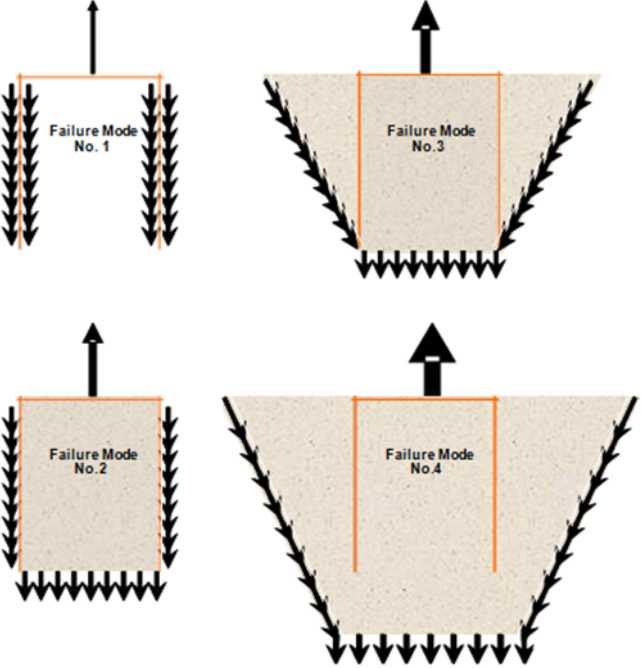


Figure 9. Free body diagrams in the soil and on the caisson at failure stage with the four main failure modes.

# 4.1. Soils (sand or clay) of low strength characteristics under drained conditions or caissons of low embedment

In general, in the current study, it has been noticed that under drained conditions suction caisson models embedded in relatively weak sands or clays perform load-displacement responses typical to that shown schematically in Figure 10.

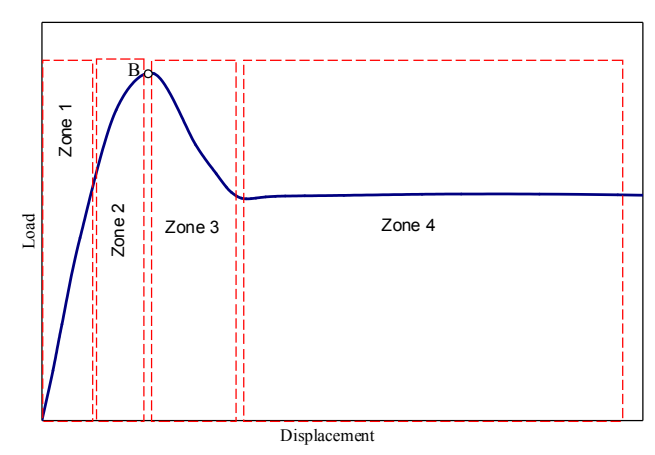


Figure 10. Schematic load-displacement response with the failure mechanism No. 1.

With small displacements (zone 1) an almost linear behaviour has been perceived. This is followed by a non-linear performance, leading to a clear ultimate pull-out load (point B in Figure 10). Then, a drop in the load turns up (zone3). This softening response ends up to a residual load bearing, which later on remains almost constant (zone 4). Figures 11 and 12 give some actual numerical results similar to this behaviour. These figures also present the effects from variations in the interface strength ratio ( $R_{int}$ ) on the pull-out response of the examined models. Regarding Figures. 11 and 12, it should be noted that in practice Kaolinite clay can hardly behave as drained unless the rate of pull-out is extremely slow or if the caisson is open-top as in the decommissioning.

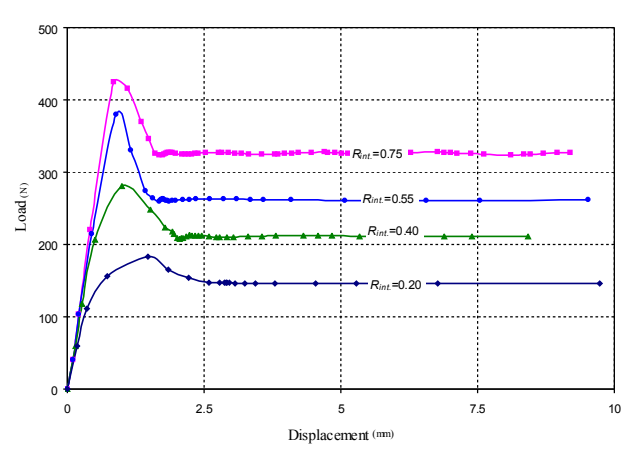


Figure 11. Failure mechanism No. 1. Typical numerical pullout response of suction caissons in weak clay under drained conditions (Kaolinite clay, drained condition, L=600 mm, D=100 mm, c=0.1 kPa,  $\varphi=27.8^{\circ}$ ,  $\psi=0$ , E=1 MPa, v=0.35).

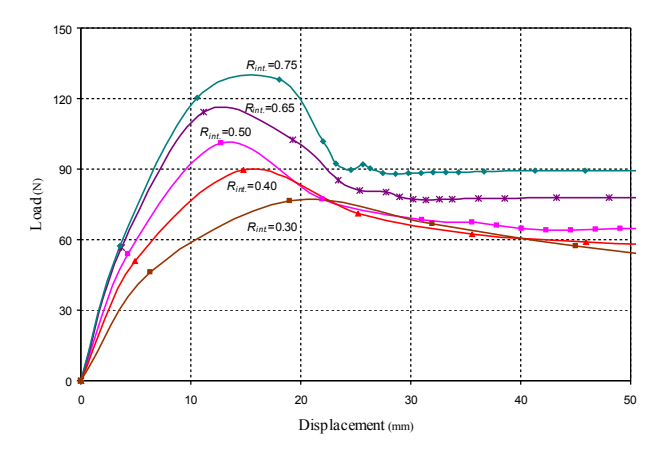


Figure 12. Failure mechanism No. 1. Typical numerical pullout response of suction caissons of low embedment in sand under drained conditions (Oklahoma sand, drained condition, L=194 mm, D=110 mm, c=0 kPa,  $\varphi=41^\circ$ ,  $\psi=11^\circ$ , E=25 MPa,  $\nu=0.3$ ).

Figure 13 shows the deformed shapes of a typical model with failure mechanism No. 1 at the end of zone 2, half way through zone 3 and in the zone 4. At similar instances, Figure 14 gives the plastic Mohr-Coulomb and tension cut-off points in the model. Figures 11 and 12 show that with this failure mode, the soil plug remains in place and the caisson moves up unaccompanied (see also Figure 9).

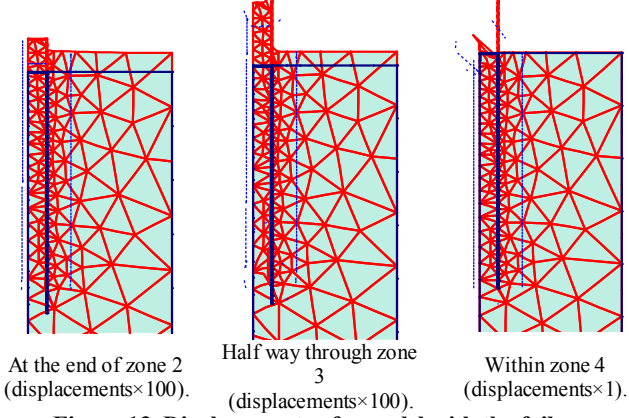


Figure 13. Displacements of a model with the failure mechanism No. 1 (model in Figure 11 with  $R_{ini}$ =0.5) at different stages of pull-out.

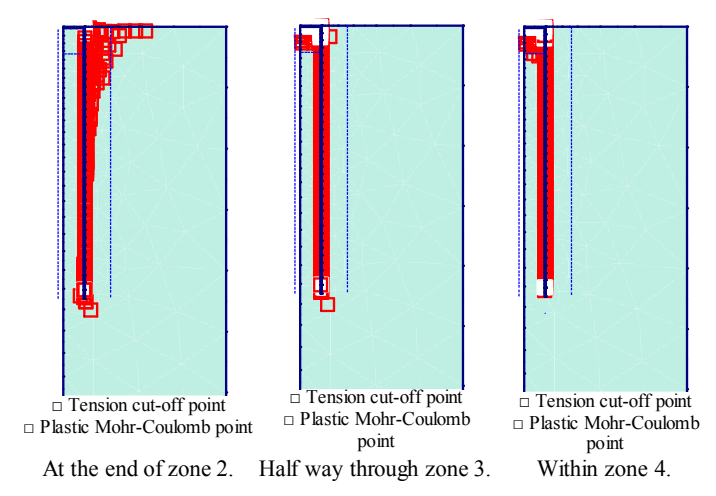


Figure 14. Plastic and tension cut-off points at different stages of pull-out in a model with the failure mechanism No. 1 (model in Figure 11 with  $R_{im}$ =0.5).

This type of failure, which occurs on the caisson side walls, is called here a local shear failure or failure mode No. 1. This is to differentiate it from other failure modes which are themselves in shear but happen in the soil body far away from the caisson walls (modes No. 3 and 4 as will be explained later). It was mentioned earlier that the load-displacement curve in Figure 10 represents a typical response of the caissons with the failure mechanism No. 1. In zones 1 and 2, the caisson's submerged weight, the soil plug's submerged weight, the reverse end bearing and the skin frictions on the caisson's skirt, all, contribute to the overall pull-out resistance. With mode No. 1 the skin friction strength on the caisson's walls appears to be lower than the summation of the reverse end bearing and the soil plug and the caisson's submerged weights. This is typical of caissons embedded in weak soils.

As the end of zone 2 (Figure 10), the soil in the immediate vicinity of the caisson's wall come close to a shear failure condition whilst the soil in the plug and the surrounding area still remain far from a yielding state. At this very point a shear failure occurs on the caisson's wall. This corresponds to the ultimate limit load in Figure 10 at the end of zone 2. Prior to this shear failure, the soil plug is sticking to the caisson in its upward movement. This means that up to point B (Figure 10) the soil plug contributes to the pull-out loading through its submerged weight and its reverse end bearing. Subsequent to the shear failure on the caisson's walls, the soil plug is left behind and does not any longer accompany the caisson in its upward movement. As a result two load bearing components (reverse tensile end resistance and the soil plug weight) are abandoned. Accordingly, a gradual drop in the pull-out load or a softening behaviour comes about (zone 3 in Figure 10). The almost uniform residual resistance (zone 4 in Figure 10) is originated from the caisson submerged weight and the yielding strength on the caissons side walls.

It should be mentioned that the failure mode No. 1 and its associated load-displacement behaviour has also been observed with caisson models of low embedment (even in soils of higher strength characteristics). For example, Figure 12 shows the results for a caisson of low penetration in sand with relatively good strength characteristics (similar to that used in Iskander et al. experiments [26]). Due to the low penetration, the average effective stress and the soil pressure at rest, which mobilizes the skin friction on the caisson walls, are trifling. In addition (with low penetrations) the caisson's skirt area is further restricted. As a result the total mobilized skin friction cannot exceed the soil plugs submerged weight plus the reversed end bearing. Consequently, once more, shear failure on the caisson's side walls takes precedence over a tensile failure in the soil plug and the failure mode No. 1 occurs.

# 4.2. Soils (sand or clay) of good strength characteristics under drained conditions

Under drained conditions and in soils with good strength characteristics, suction caisson models have been found to commonly present load-displacement responses typical to that shown in Figure 15. Zone 1 in the figure virtually renders a linear behaviour (generally for displacements up to 2% of the caisson length). This is followed by a non-linear response (zone 2) which ends up to an ultimate limit load. Subsequently, with increase in the displacement (zone 3), the load remains almost unchanged. Some actual outcomes typical to this behaviour from the models studied are given in Figure 16. This figure also shows the caisson widening effects (increase in D while L is constant) on the pull-out response of these models [30].

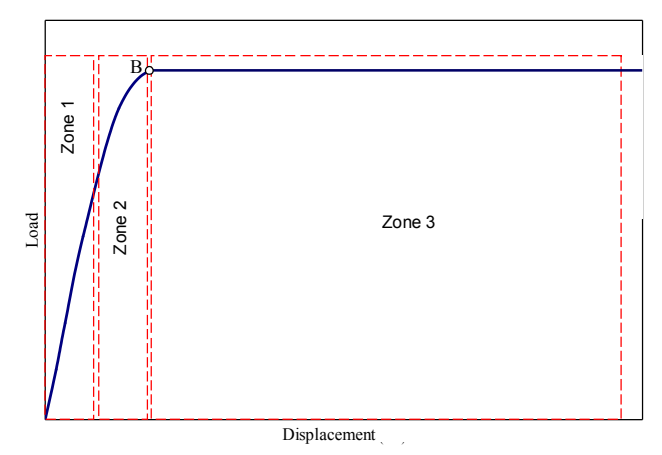


Figure 15. Schematic load-displacement response with the failure mechanism No. 2.

Figures 15 and 16 show the model status at the end of zone 1, in zone 2 just prior to the ultimate pull-out load, and within zone 3. As it can be noticed, with this failure mechanism a tensile failure is developed in the soil plug close to the caisson's tip. Subsequent to this failure, the detached soil plug comes up along with the caisson (see also Figure 9).

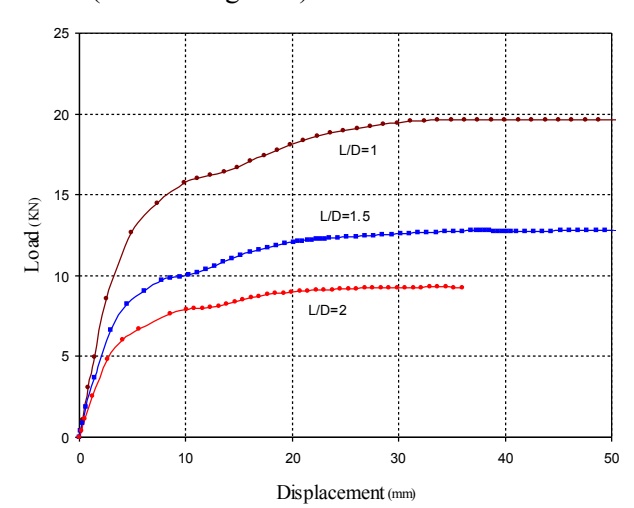


Figure 16. Failure mechanism No. 2. Typical numerical pullout response of suction caissons in clay under drained conditions (Kaolinite clay, drained condition, L=600 mm, D=variable, c=1.5 kPa,  $\varphi=27.8^{\circ}$ ,  $\psi=0$ , E=1.5MPa, v=0.35).

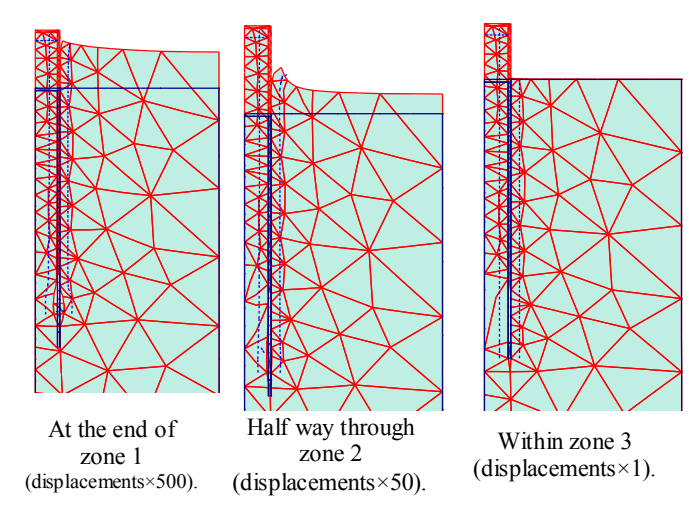


Figure 17. Deformations of a model with the failure mechanism No. 2 at different stages of pull-out (model in Figure 16 with L/D=6).

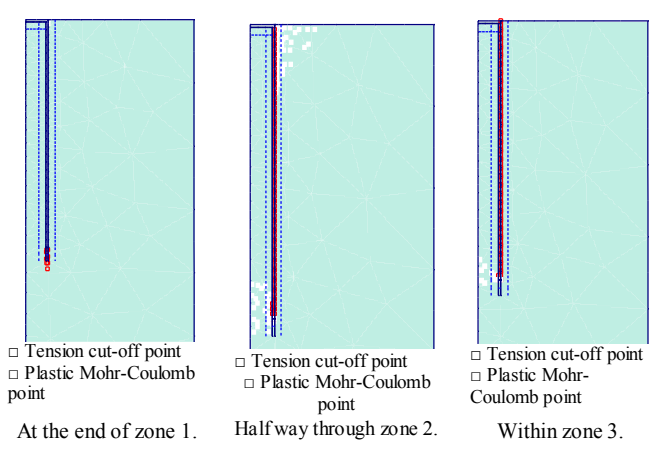


Figure 18. Plastic and tension cut-off points at different stages of pull-out in a model with the failure mechanism No. 2 (model in Figure 16 with L/D=6).

Figures. 17 and 18 show the deformed shapes of a typical model and the plastic Mohr-Coulomb and tension cut-off points in the model with failure mechanism No. 2. Soils of this category are of better strength characteristics than those soils with the failure mode No. 1. It means that dissimilar to the first category, the resistance component from skin friction surpasses those from the submerged soil plug weight plus the reversed end bearing capacity. So at some stages (within zone 2) the soil plug initiates a tensile failure around its lower end, while the skin friction strength on the caisson walls is yet far from yielding. Later on, as the soil plug gradually separates from the underlying soil, extra loads are redistributed on the caisson's outer skin. This exacerbates the load bearing situation on the outer skin and speeds up a shear yielding on this surface. Highly non-linear performance at the end of zone 2 (Figures 13 and 14) seems to justify the mentioned circumstances.

The ultimate load at the end of zone 2 coincides with a shear yielding state on the outer skin of the caisson. Afterward, as the pull-out advances, no further significant developments in the load bearing conditions are anticipated. Therefore the pull-out load has been observed to stay almost constant within zone 3, as a residual resistance.

This type of failure (failure mode No. 2) is called here a local tensile failure mode. This is to differentiate it from other types of failure which are in shear (modes No. 1, 3 and 4) and those which are global and occur far away from the caisson (modes No. 3 and 4).

In general, it has been noticed that with improvement in the soil characteristics, the failure mode shifts from No. 1 to No. 2 and accordingly higher pull-out capacities are achieved. This has been noticed, for example, when  $\phi$  or c values have been gradually increased from low values to higher values.

#### 4.3. Clays under undrained conditions

With clays under undrained conditions, suction caisson models have been found to mainly perform load-displacement responses similar to that schematically presented in Figure 19. As before, zone 1 remains almost linear. The non-linear performance in zone 2 is followed by a low slope hardening response.

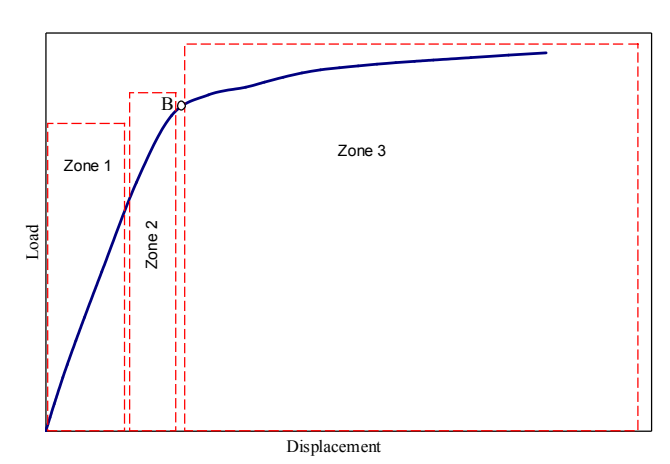


Figure 19. Schematic load-displacement response with the failure mechanism No. 3.

This hardening behaviour discerns the response in this category from that of the second failure mechanism. With this category, dissimilar to categories 1 and 2, there exists no apparent ultimate load. With this failure mechanism the ultimate load has then been chosen as the minimum of two. The first one corresponds to the intersection of the lines overlying the responses in zone 1 and the hardening responses in zone 3. The second load is associated to caissons displacement of 0.25L as recommended by Rao et al. [11].

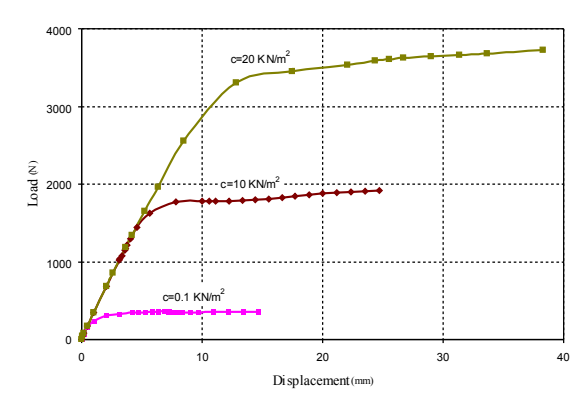
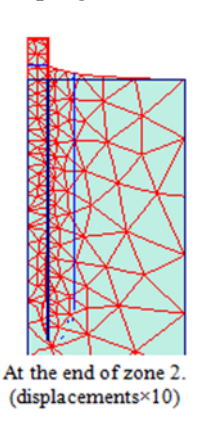


Figure 20. Failure mechanism No. 3. Typical numerical pullout response of a suction caisson in clay under undrained conditions (Kaolinite clay, undrained condition, L=600 mm, D=100 mm, c=variable,  $\varphi=27.8^{\circ}$ ,  $\psi=0$ , E=1.5 MPa, v=0.35).

Figure 20 gives some results obtained from suction caisson models in clay under undrained conditions. This figure also demonstrates the soil cohesion effects on the pull-out response of the model.

For one model of this category, Figures 19 and 20 demonstrate the deformations and the yielding status, at the end of zones 2 and within zone 3 respectively. By the end of zone 3, a tensile failure occurs at lower sections of the soil plug. This is in conjunction to a shear failure in the soil surrounding the caisson. The shear failure surface has been noticed to partially coincide with the lower parts of the caisson's outer skin. Then about half way through the caisson wall, it extends out to the soil surface forming a local failure wedge in the vicinity of the caisson (see Figure 9). Figures 21 and 22 show the deformed shapes of a typical model and the plastic Mohr-Coulomb and tension cut-off points in the model with failure mechanism No. 3. Figure 22 indicates that the shear failure takes precedence over the tensile failure in the soil plug.



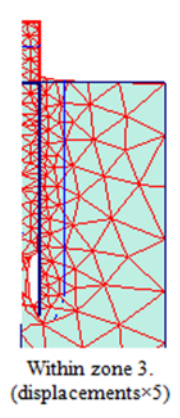
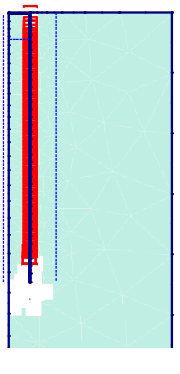


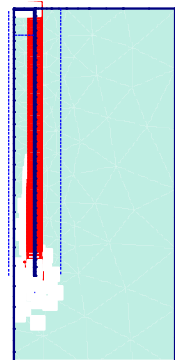
Figure 21. Deformations of a model with the failure mechanism No. 3 at different stages of pull-out (model in Figure 20 with c=20 kPa).

Pull-out loads generate negative pressures (suction) inside an undrained caisson. The suction develops beneath the caisson cap, in the soil plug and partially extends itself into the surrounding soil. Direct and indirect suction effects cause higher effective stresses,

create seepage forces and strengthen the bonding between the inner skin of the caisson with the soil latter. enhances the resistance characteristics on interfaces of the soil plug both with the inner skin and with the soil underneath the caisson. Due to direct effects of the suction and the seepage forces, a tension failure similar to that observed with failure mode 2 is postponed to the later stages of the loading. Therefore, neither a premature local shear nor a local tensile failure identical to those reported for failure modes 1 and 2 occur. With the current category of "soil/caisson/drainage", the failure is extended to the outer soils. This can be regarded as the contribution of the suction developed under an undrained condition (see Figure 9).

Under undrained conditions, suction effects in clays are restricted to the immediate outer soil. This is due to the low permeability of clay. Therefore, failure surfaces in the surrounding soil stay quite close to the caisson and even partially overlap the lower part of the caisson (Figure 22). This is in contrast to the suction caissons in sand under undrained conditions where, as will be illustrated later, the failure surfaces are extended well away from the caisson.





At the end of zone 2.

Within zone 3

Figure 22. Plastic and tension cut-off points at different stages of pull-out in a model with the failure mechanism No. 3 (model in Figure 20 with c=20 kPa).

As reported earlier, formation of the mentioned failure wedge in the outer soil is followed by a tensile failure at the lower part of the soil plug. With further displacements, unlike to the drained models, the pull-out load still increases but has a low rate.

The hardening behaviour seems an outcome of the suction which is typical of undrained conditions. Extra displacement beyond point B boosts up the suction. This leaves a growing effect on the pull-out load. This is a direct effect from the suction in zone 3. The increase in the suction also augments the effective stresses on the yield surface formed outside the caisson. It causes expansions to the yield surfaces in the plasticity model. Therefore, even staying in a yielding status, the overall shear accumulated over failure surfaces, keeps mounting with the increase in the suction. This is an indirect effect from the suction in zone 3.

As mentioned above, due to the low permeability of clays, the suction inserts limited effects within the outer soil. With undrained clay models, the increase in the load bearing in zone 3 (the hardening performance) seems to be mostly caused by direct effects from the suction rather than from indirect improvements in the plastic behaviour of the soil. This appears to explain why beyond point B the load bearing is increasing and why it has a trivial rate.

The failure surface in the surrounding soil is partially located on the caissons outer skin and partially lays on the lower face of a failure wedge (see Figure 9). It has been noticed that, under undrained conditions, with clays of lower cohesion the upper wedge grows smaller. In these cases the failure mechanisms has been observed to gradually move from a typical mode 3 to a failure mode 2 (see also Figure 9).

## 4.4. Sands under undrained conditions

Models of suction caissons in sands under undrained conditions have mostly been found to perform load-displacement responses similar to that of undrained clays. The main difference is that the response in zone 3 (the hardening zone) has a higher slope (Figure 23).

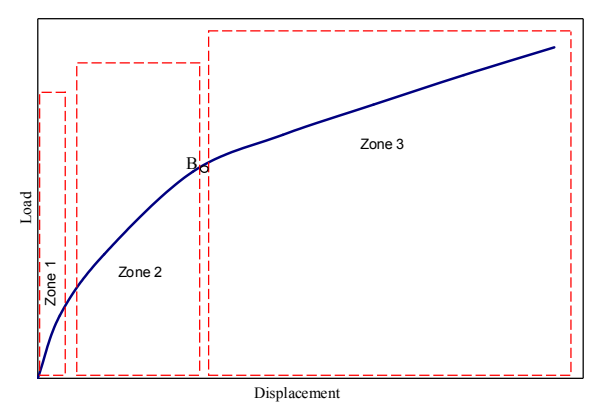


Figure 23. Schematic load-displacement response with the failure mechanism No. 4.

As discussed previously, the hardening performance within zone 3 has been found to be distinctive of undrained models. It is most likely caused by direct and indirect effects from the suction build up inside the caisson when subjected to the pull-out loads. Higher permeability in sand likely intensifies the indirect effects from the suction. This presents itself as a steeper hardening response in zone 3, in comparison to the clay models. In some cases the slopes in zone 2 and 3 have been observed to become almost identical. Figure 24 shows some of the actual results obtained for this "soil/caisson/drainage" category. The figure also shows the soil internal friction angle effects on the pull-out response of the examined model. It should be mentioned that the hardening performance in zone 3 may also partially be a product of the dilatancy angle  $(\psi)$  considered for modelling of dense sands [31].

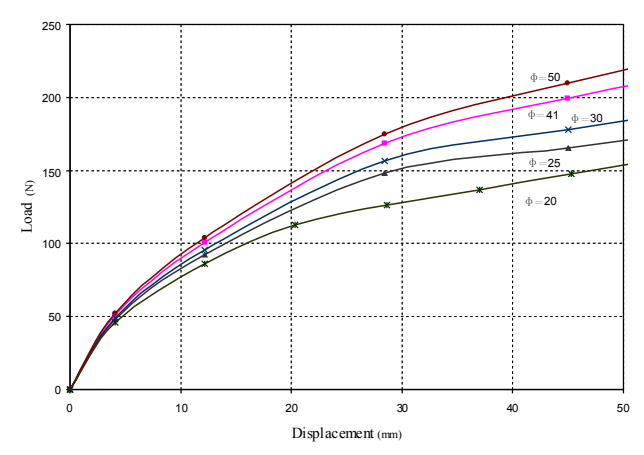


Figure 24. Failure mechanism No. 4. Typical numerical pullout response of suction caissons in sand under undrained conditions (Oklahoma sand, undrained condition, L=194 mm, D=110 mm, c=0 kPa,  $\varphi=$ variable,  $\psi=\varphi$  -30° for  $\varphi>$ 30°,  $\psi=$ 0° for  $\varphi\leq$ 30°, E=25 MPa, v=0.3).

Figures. 25 and 26 display deformations and the yielding status for one typical model at the end of zones 2 and within zone 3 respectively. These figures indicate on a fourth type of failure mode with this "soil/caisson/drainage" category. The failure surface is now well extended into the soil surrounding the caisson (see also Figure 9). This is called here a global shear failure mode. The global shear failure is accompanied with the bed subsidence at far end of the soil model. Once more, it appears that higher permeability of the sand has allowed the suction to spread out its effects well into the surrounding soil. Therefore, even though in shear, the failure is global as compared with undrained clays where the failure was somewhat local and close to the caisson itself. It is noted that the Plaxis model used in the current study does not allow for the coupled hydro-mechanical analysis of the suction caisson pull-out. Therefore the discussions made in this Section on the effects from higher permeability of sand need to be further substantiated using a fully coupled hydro-mechanical soil modelling.

It should be mentioned that in general it has been noticed that the suction caisson pull-out capacity increases with the order of the above described failure modes No. 1 to 4. In other words, higher pull-out capacities can be achieved with the extent that the failure mechanism shifts from local to global modes. Another important observation is that low penetration causes the caisson to fail in lower and more local failure modes.

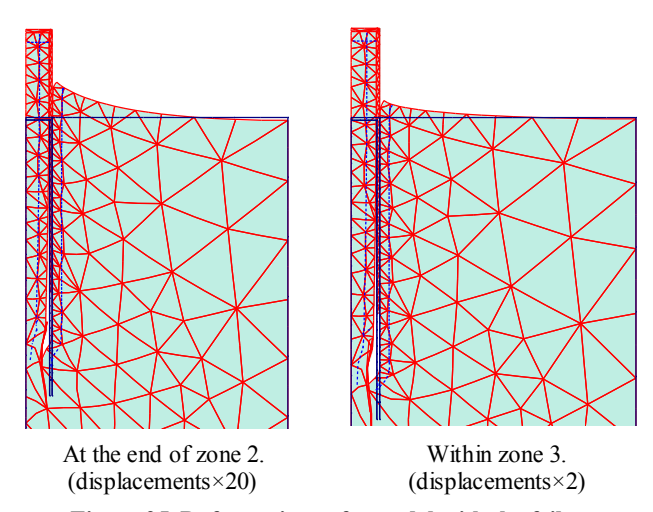


Figure 25. Deformations of a model with the failure mechanism No. 4 at different stages of pull-out (sand, undrained condition, L=600 mm, D=100 mm, c =0 kPa,  $\varphi$  =41°,  $\psi$ = 11°, E=25 MPa,  $\nu$ =0.3).

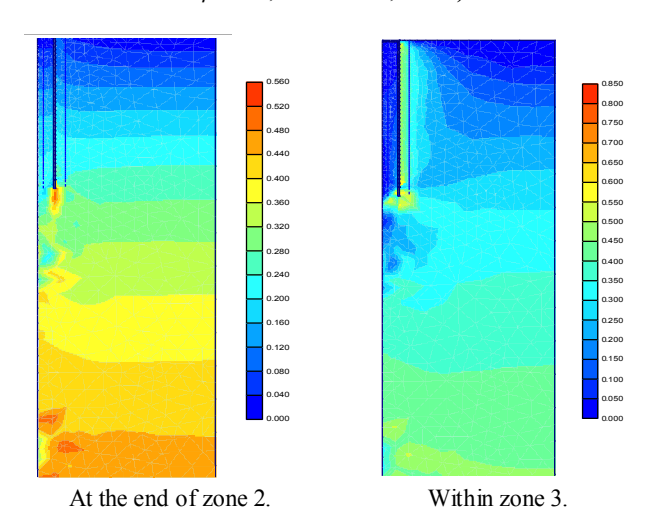


Figure 26. Relative shear stresses at different stages of pull-out in a model with the failure mechanism No. 4 (sand, undrained condition, L=600 mm, D=100 mm, c =0 kPa,  $\varphi$  =41°,  $\psi$ = 11°, E=25 MPa, v=0.3).

It should be mentioned that the failure mechanisms and the "soil/caisson/drainage" categories assigned in this paper for each failure mode are ascertained through a numerical investigation. This still needs to be further supported by experiments particularly aimed at defining the failure mechanisms of suction caissons. The categories assigned for each failure mode are based on the general trends found with the models. There have also been failure modes not exactly following the general "soil/caisson/drainage" classifications presented above.

It is noted that in general soils of high strength (high density) such as dense sands and stiff clays tend to demonstrate a softening behaviour beyond experiencing a peak strength in their load-deformation response. On the other hand, low strength soils such as loose sands and soft clays tend to demonstrate a hardening behaviour with no distinct peak in their response [32]. Figs 8 and 13 do not reflect above mentioned classical trends. This is most probably because several mechanisms, such as the

shear behaviour of the soil layers in the vicininty of the caisson wall, the reverse end bearing, the caisson weight, the plug weight, the oveal resistance of the soil around the caisson and more decisively the suction effects are involved. While one mechanism is experiencing a softening behavioue other mechanisms may still demostrating hardening behaviour. The overal pull-out response is an outcome of contributions from all mechanisms involved and the sequence of failure modes.

As an example, when the top of the caisson is sealed, the water inside the caisson will be trapped, the situation can be assumed as fully undrained. With caissons of sufficient embedment, the suction effects dominates the pull-out resistance. The contribution from the suction to the overal ressistance increases by the increase in the pull-out, even beyound the point the dense sands or stiff clays have reached their peak strengths.

When the top of the caisson is unsealed, the situation can be assumed as fully drained. There will be then no contribution from the suction. In cases where the failure in the reverse end bearing prevails other failure modes, the load displacement curve will first experience a drop upon the loss of the reverse end bearing. Beyond this drop in the load bearing, the load-displacement curves in soils of low strength (e.g. Figure 10) proceed with a low hardening response.

# 5. Conclusions

In this paper results from a numerical investigation on failure mechanisms of suction caissons under vertical pull-out loads are reported. It gives relatively detailed information on the calibration and verification of the numerical model of suction caissons against experimental data from other researches. An acceptable level of correspondence has been observed between the numerical and experimental results. Verified numerical models have then been employed to obtain the pull-out response of suction caissons under a variety of conditions.

In the current research, as a key finding, four distinctive failure modes are introduced for the vertical pull-out of suction caissons. They vary from local modes, with caissons of low penetration in weak soils under drained conditions, to global modes, with caissons of sufficient penetration in stronger soils under undrained conditions.

The first failure mode corresponds to caissons of low penetration or those embedded in weak soils under drained conditions. A local shear failure has been noticed to transpire with this category. The second mode is in general related to caissons in soils with good strength characteristics under drained conditions. They have been found to show a local tensile failure. The third category is mostly associated with suction caissons in clays under undrained conditions. They demonstrate a minor hardening behaviour and exhibit

a partially global shear failure. The forth category typically characterizes suction caissons in sands under undrained conditions. They have been found to present a distinct hardening response and fail in a global shear mode.

In general, with local modes the failure surface is close to caisson walls. With global modes, the failure surface moves away from the caisson walls and well extends in the surrounding soil. The pull-out capacity is highly reliant on the mode of the failure and on the whole it increases as the mode moves from local to global. Suction caissons of low penetration have been noted to fail in lower and more local failure modes.

# Acknowledgment

The authors would like to thank the anonymous reviewer for his/her valuable comments and suggestions which we believe substantially improved the quality of the manuscript.

# **List of Symbols**

c:soil cohesion $\varphi$ :soil friction angle $\psi$ :soil dilatancy angle $\gamma$ :soil wet unit weight $\gamma_{d \text{ max}}$ :maximum dry unit weight $\gamma_{d \text{ min}}$ :minimum dry unit weight

G<sub>s</sub>: specific gravity
 v. Poisson's ratio
 c<sub>u</sub>: undrained cohesion
 C<sub>c</sub>: coefficient of curvature
 C<sub>u</sub>: uniformity coefficient
 S<sub>r</sub>: degree of saturation
 E: Young's modulus of elasticity

 $e_{max}$ : maximum voids ratio  $e_{min}$ : minimum voids ratio

PL: plastic limit
LL: liquid limit
LI: liquidity index

 $R_{int}$ : soil-caisson interface coefficient

L: caisson length
D: caisson diameter
L/D: aspect ratio

t: caisson wall thickness

# 7. References

- 1- LeTirant, P., (1979), Seabed reconnaissance and offshore soil mechanics for installation of petroleum structures. Gulf Publishing Company, Texas.
- 2- Maniar, D.R., Vásquez, L.F.G and Tassoulas, J.L., (2005) *Suction caissons: finite element modeling*. Proceedings of 5<sup>th</sup> GRACM International Congress on Computational Mechanics Limassol.
- 3- Bakker, T.T., de Heer, M.A., Heerema, A.E. and Smeets, P., (2006), *Theory of a vertically loaded Suction Pile in Clay*, TU Delft University.
- 4- Zeinoddini, M., Kakasoltani, S., Abdi, M. R., & Ahmadi, I. (2014). *Model testing of upright and tapered suction caissons in sand*, Journal of Ships and Offshore Structures.

- 5- Zeinoddini, M., Keyvani, J. and Nabipour M., (2011), *Wall slope effects on the vertical pull-out capacity of tapered suction caissons*, Elsevier Journal of Scientia Iranica, Transactions A: Civil Engineering, Vol.18, p.313-325.
- 6- Tjelta, T.I., (1995), Geotechnical experience from the installation of the Europipe jacket with bucket foundations, Proceedings, Offshore Technology Conference, OTC 7795, p. 897-908.
- 7- Clukey, E.C., Morrison, M.J., Gariner, J. and Corté, J.F., (1995), *The response of suction caissons in normally consolidated clays to cyclic TLP loading conditions*, Proceedings, Offshore Technology Conference, p. 909-918.
- 8- Randolph M.F., (2002), *Analysis of suction caisson capacity in clay*, Proceedings, Offshore Technology Conference, Houston, Texas, USA.
- 9- Thieken, K., Achmus, M., and Schröder, C, (2014), On the behavior of suction buckets in sand under tensile loads. Computers and Geotechnics, 60, p.88-100.
- 10- Steensen-Bach, J.O., (1992), Recent model tests with suction piles in clay and sand. Proceedings, Offshore Technology Conference, OTC 6844, p. 323-330.
- 11- Rao, S.N.. Ravi, R. and Ganapathy, C., (1997), *Pullout behavior of model suction anchors in soft marine clays*, Proceedings, Seventh International Offshore and Polar Engineering Conference, Honolulu.
- 12- Whittle, A.J., Germaine, J.T. and Cauble, D.F., (1998), *Behavior of miniature suction caissons in clay*, Offshore Site Investigation and Foundation Behaviour '98, SUT, p. 279-300.
- 13- El-Gharbawy, S. and Olson, R.E., (1999), Suction caisson foundations in the Gulf of Mexico. Analysis, Design, Construction, and Testing of Deep Foundations. ASCE Journal of Geotechnical Engineering, Vol.88, p.281-295.
- 14- Byrne, B.W. and Houlsby, G.T., (2002), Experimental investigations of response of suction caissons to transient vertical loading, Journal of Geotechnical and Geoenvironmental Engineering, Vol. 128, p. 926-939.
- 15- Zeinoddini, M., Mousavi, S. A., & Abdi, M. R. (2011), Simulation of suction caisson penetration in seabed using an adaptive mesh technique, Procedia Engineering, Vol.14, p.1721-1728.
- 16- Zeinoddini, M. Keyvani, J. and Nabipour M., (2009), *Tapered suction caissons: a numerical investigation into their pull-out performance*, International Journal of China Ocean Engineering Vol.23, No.4, p. 695-707.
- 17- El-Gharbawy, S.L. and Olson, R.E, (2000). *Modeling of suction caisson foundations*, Proceedings of the International Offshore and Polar Engineering Conference, Vol. 2, p. 670-677.

- 18- Deng, W. and Carter, J.P., (2002), A theoretical study of the vertical uplift capacity of suction caissons, International Journal of Offshore and Polar Engineering, Vol. 12, p.89-97.
- 19- Simulia (2009), Abaqus User Manual, version 6.10, Dassault Systèmes Simulia Corp., Providence, RI, USA,
- 20- Brinkgreve, R.B.J., (2000) PLAXIS ver. 7.2, user manual, finite element code for soil and rock analyses. Delft University of Technology, A.A. Balkema Publishers.
- 21- Smith, I.M. and Griffith, D.V., (1982). *Programming the finite element Method*, Second Edition. John Wiley & Sons, Chisester, U.K.
- 22- Davie, J.R. and Sutherland, H.B, (1978), *Modeling of clay uplift resistance*, ASCE Journal of Geotechnical Engineering, Vol.104 (GT6), p. 356-360.
- 23- Rao, S.N., Prasad, B.S. and Veeresh, C., (1993), *Behaviour of embedded model screw anchors in soft clays*. Journal of Geotechnique, Vol.43, p.605-614.
- 24- Dekker, M. J., (2014). *The Modelling of Suction Caisson Foundations for Multi-Footed Structures*, MSc thesis, Delft University of Technology and Norwegian University of Science and Technology.
- 25- El-Gharbawy, S. and Olson, R.E., (1998), *The pullout capacity of suction caissons for tension leg platforms*, Proceedings of 8<sup>th</sup> International Offshore and Polar Engineering Conference, Montreal.

- 26- Iskander, M., El-Gharbawy, S. and Olson, R., (2002). *Performance of suction caissons in sand and clay*, Canadian Geotechnical Journal, Vol.39, p.576-584.
- 27- Edgers, L., Andresen, L., & Jostad, H. P., (2009), Capacity analysis of suction anchors in clay by 3D finite element analysis. Plaxis Bulletin No. 24.
- 28- Zeinoddini, M., Saeidi, B., & Parke, G. A. R. (2008), Feasibility of Suction Caisson Solutions for the Foundations of Offshore Jacket Platforms in the Persian Gulf. In ASME 2008 27<sup>th</sup> International Conference on Offshore Mechanics and Arctic Engineering, p. 519-525.
- 29- Supachawarote, C., Randolph, M., and Gourvenec, S. (2004), *Inclined pull-out capacity of suction caissons*, In The 14<sup>th</sup> International Offshore and Polar Engineering Conference.
- 30- Zeinoddini, M. and Nabipour M., (2006), *Numerical investigation on the pull-out behaviour of suction caissons in clay*, The 25<sup>th</sup> International Conference on Offshore Mechanics and Arctic Engineering OMAE2006.
- 31- Nedderman, R.M., (1992), *Statics and Kinematics of Granular Materials*. Cambridge University Press, ISBN 0-521-01907-9.
- 32- Terzaghi, K., Peck, B. R., and Mesri, G., (1996), *Soil Mechanics in Engineering Practice*, 3rd ed., Wiley, New York, p. 71-213.